GA–A24862

DEVELOPMENT, PHYSICS BASIS, AND PERFORMANCE PROJECTIONS FOR HYBRID SCENARIO OPERATION IN ITER ON DIII-D

by
M.R. WADE, T.C. LUCE, R.J. JAYAKUMAR, P.A. POLITZER,
A.W. HYATT, J.R. FERRON, C.M. GREENFIELD, E.H. JOFFRIN,
M. MURAKAMI, C.C. PETTY, R. PRATER, J.C. DeBOO, R.J. LA HAYE,
P. GOHIL, T.L. RHODES, and A.C.C. SIPS

OCTOBER 2004

DISCLAIMER

GA–A24862

DEVELOPMENT, PHYSICS BASIS, AND PERFORMANCE PROJECTIONS FOR HYBRID SCENARIO OPERATION IN ITER ON DIII-D

by
M.R. WADE,* T.C. LUCE, R.J. JAYAKUMAR,† P.A. POLITZER, A.W. HYATT, J.R. FERRON, C.M. GREENFIELD, E.H. JOFFRIN,‡ M. MURAKAMI,* C.C. PETTY, R. PRATER, J.C. DeBOO, R.J. LA HAYE, P. GOHIL, T.L. RHODES,Δ and A.C.C. SIPS#

This is a preprint of a paper to be presented at the 20th IAEA Fusion Energy Conference, Vilamoura, Portugal, November 1–6, 2004 and to be published in the *Proceedings.*

*Oak Ridge National Laboratory, Oak Ridge, Tennessee.
†Lawrence Livermore National Laboratory, Livermore, California.
‡CEA Cadarache Euratom Association, Cadarachhe, France.
ΔUniversity of California – Los Angeles, Los Angeles, California.
#Institut fur Plasmaphysik, Garching, Germany.

Work supported by
the U.S. Department of Energy
under DE-AC05-00OR22725, W-7405-ENG-48,
DE-FC02-04ER54698 and DE-FG03-01ER54615

GENERAL ATOMICS PROJECT 30200
OCTOBER 2004

Development, Physics Basis, and Performance Projections for Hybrid Scenario Operation in ITER on DIII-D

M.R. Wade,[1] T.C. Luce,[2] R.J. Jayakumar,[3] P.A. Politzer,[2] A.W. Hyatt,[2] J.R. Ferron,[2] C.M. Greenfield,[2] E.H. Joffrin,[4] M. Murakami,[1] C.C. Petty,[2] R. Prater,[2] J.C. DeBoo,[2] R.J. La Haye,[2] P. Gohil,[2] T.L. Rhodes,[5] and A.C.C. Sips[6]

[1]Oak Ridge National Laboratory, Oak Ridge, Tennessee, USA
[2]General Atomics, P.O. Box 85608, San Diego, California 92186-5608, USA
[3]Lawrence Livermore National Laboratory, Livermore, California, USA
[4]CEA Cadarache Euratom Association, Cadarache, France
[5]University of California-Los Angeles, Los Angeles, California, USA
[6]Institut fur Plasmaphysik, Garching, Germany

e-mail contact of main author: wade@fusion.gat.com

Abstract. A new standard in stationary tokamak performance is emerging from experiments on DIII-D. These experiments have demonstrated the ability to operate near the free boundary, n=1 stability limit with good confinement quality under stationary conditions. The normalized fusion performance is at or above that projected for Q_{fus} = 10 operation in the International Thermonuclear Experimental Reactor (ITER) design over a wide operating range in both edge safety factor (3.2–4.5) and plasma density (35%-70% of the Greenwald density). Projections to ITER based on this data is uniformly positive and indicate that a wide range of operating options may be available on ITER, including the possibility of sustained ignition. Recent experiments have demonstrated the importance of a small m=3, n=2 neoclassical tearing mode in avoiding sawteeth and the effect of edge localized modes on tearing mode stability at an edge safety factor near 3. Transport studies using the GLF23 turbulence transport code indicate that ExB stabilization is important in reproducing the measured profiles in the simulation. Yet, even in cases in which the toroidal rotation is low, confinement quality is robustly better than the standard H-mode confinement scalings.

1. Introduction

Over the past decade, fusion confinement research has focused on the characterization of the H-mode confinement regime, seeking to quantify plasma behavior in this regime sufficiently well that extrapolations from present-day devices to next generation devices such as the International Thermonuclear Experimental Reactor (ITER) can be made with a reasonable degree of confidence [1]. While this characterization has provided reasonable confidence that ITER can achieve its mission of $Q_{fus} = P_{fus}/P_{input} = 10$ operation, a new standard in plasma performance for stationary tokamak operation is emerging from recent experiments on the DIII-D tokamak [2-4] and other tokamaks [5-7]. The DIII-D experiments have demonstrated stationary ($t_{dur} > 35\tau_E > 3\tau_R$) plasma operation at high β (within 0-20% of the free boundary, ideal n = 1 stability limit) and with good confinement quality (20%-50% better than the standard confinement scalings for H-mode). The operation space over which this level of performance can be sustained has been shown to be quite large, including a wide range of density ($0.35 < n_e/n_{GW} < 0.7$) and edge safety factor ($2.8 < q_{95} < 4.5$). Projections based on these results towards ITER indicate that that this operating regime offers many operation options not presently envisaged for ITER, ranging from long-pulse, high neutron fluence operation (Q_{fus} = 5 for 5000 s) to very high fusion gain operation ($Q_{fus} > 40$). This operating regime has been dubbed the "hybrid" regime by working groups of the International Tokamak Physics Activity (ITPA) due to the ability to sustain stationary performance at levels approaching that possible in Advanced Tokamak (AT) scenarios but without significant bootstrap current (and thus incapable of steady-state operation). While the physics basis of this regime is still being developed, considerable insight into access, sustenance, and the basic characteristics of these plasmas have been garnered from dedicated experiments. In this paper, we will present the attained performance in this regime and the operation space over which it has been obtained, key components of this physics basis, and projections to ITER based on these results.

The DIII-D hybrid regime shares many of the same characteristics as the conventional H-mode regime. Yet, there are some striking differences. The most prominent of these is the observed m=1, n=1 behavior. In the conventional H-mode case, sawteeth are ubiquitous, determine to a large extent the physics inside the sawtooth inversion radius, and can have deleterious effects on overall plasma performance [e.g., triggering of neoclassical tearing modes (NTMs)]. The present ITER design [8] is driven strongly by this latter effect with the normalized beta β_N limited ~50% below the free boundary, ideal n=1 stability limit (denoted by $\beta_N^{no-wall}$). Here, $\beta_N = \beta/\left(I_p/aB_T\right)$, $\beta = 2\mu_o\langle p\rangle/B_T^2$, $\langle p\rangle$ is the average kinetic pressure, I_p is the plasma current, a is the plasma minor radius, and B_T is the toroidal magnetic field. In contrast, sawteeth are either absent or very small in the hybrid regime and therefore play little role in either the transport/stability physics or the overall performance of the regime. The lack of sawteeth leads to a higher stability limit and robust operation with the sustainable β_N being 80%-100% of $\beta_N^{no-wall}$. Confinement in the hybrid regime is also observed to be better than the standard H-mode scaling law predictions over the entire operation space, which serves as the basis for the ITER baseline scenario. The combination of improved stability and confinement in the hybrid regime project to significantly higher values of Q_{fus} in ITER. The attainable value of Q_{fus} in a fusion device is determined, to first order, by the parameter $G \equiv \beta_N H_{89}/q_{95}^2$ [3] where H_{89P} is the confinement quality relative to L-mode scaling law prediction [9]. For the ITER baseline scenario, $\beta_N = 1.8, H_{89P} = 2.1$, and $q_{95} = 3$, the latter driven by the increased risk of large disruptions at $q_{95} < 3$. To achieve $Q_{fus} = 10$ operation in ITER under these constraints, extremely high plasma currents (in excess of 14 MA) are required. While the ITER engineering design appears capable of handling such plasma currents, the duration over which $Q_{fus} = 10$ can be sustained is only 400 s, possibly limiting certain physics studies since the resistive current diffusion time in ITER is expected to be quite long. A convenient measure of the plasma duration is $N_{\tau_R} = t_{dur}/\tau_R$. Here, t_{dur} is the duration over which high performance is maintained and $\tau_R(s) \equiv 0.171\, R/\Re$ is the diffusive time for the lowest radial moment of the current profile at constant current, where R is the plasma major radius in m and $\Re$ is the plasma resistance in μΩ [10]. Given the current engineering design for ITER, $N_{\tau_R} \approx 2$ in a full length $Q_{fus} = 10$ standard baseline scenario pulse.

The results described here could possibly open up a much larger set of operating options in ITER. The improved values of β_N and H_{89P} result in a significant improvement over the ITER baseline scenario at $q_{95} = 3.2$ while the same value of G has been obtained at $q_{95} = 4.5$. Projections to ITER based on the obtained data are uniformly positive. Details of these projections are presented later. In terms of both normalized performance G and normalized duration N_{τ_R}, the results from DIII-D significantly exceed that of ITER as is exemplified by Fig. 1. Note that the discharges represented at the far right-hand side of this figure are all terminated due to hardware constraints and not plasma physics considerations.

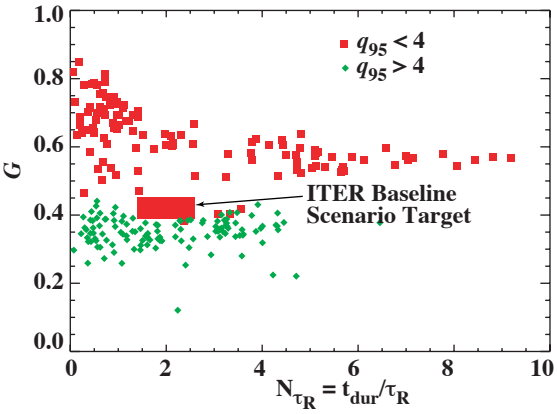

Fig. 1. Ignition figure of merit ($\beta_N H_{89P}/q_{95}^2$) versus the sustained duration relative to the resistive diffusion time (τ_R) for a series of hybrid discharges.

2. Operating Space and Projections

A representative discharge for this regime is shown in Fig. 2. Plasma parameters are: I_p = 1.2 MA, B_T = 1.7 T, q_{95} = 3.2, and $\bar{n}_e = 5\text{x}10^{19}$ m^{-3}. As is typical of these discharges, moderate neutral beam injection (NBI) power is applied during the current ramp-up phase to obtain a nearly flat q profile at end of the current ramp-up. The NBI power is then increased briefly to obtain reliable H-mode access and then

actively controlled via feedback on β_N for the remainder of the discharge. In this case, an average NBI power of 4.3 MW is required to maintain $\beta_N = 2.6$. Shortly after the high β phase begins, a small m=3, n=2 neoclassical tearing mode (~7-8 G at the wall) is triggered followed shortly by small, periodic m=1, n=1 sawteeth. As will be discussed later, these sawteeth are generally only seen with $q_{95} < 4$ in this regime. Detailed analysis of the plasma profiles (both kinetic and magnetic) indicates that the plasma pressure and current profiles are truly stationary. The sustained performance in this case is impressive with $\beta_N = 2.7$, $H_{89P} = 2.3$ being maintained for over 9.5 s, translating to $G = 0.6$ and $N_{\tau_R} = 9$. Details of the key control features and evolution of this class of discharges have been discussed previously [2-4,11].

In response to requests by the ITPA Steady-State and Transport Working Groups, dedicated experiments have been carried out over the past few years to determine the extent of the existence domain of this operating regime. Because of the strong sensitivity of fusion performance on q_{95}, studies have been conducted to determine the dependence of attainable performance as q_{95} is varied [3], the results of which are shown in Fig. 3. This was done by maintaining a constant plasma current while varying the toroidal field from $B_T = 1.85$ T ($q_{95} = 4.6$) to $B_T = 1.2$ T ($q_{95} = 3.2$). These scans have revealed two classes of discharges based on the value of q_{95} — the first class has $q_{95} > 4$ with no sawteeth while the second class has $q_{95} < 4$ with small sawteeth. For cases with $q_{95} > 4$, operation with $\beta_N \approx \beta_N^{\text{no-wall}}$ is routinely obtained. Studies have shown that this limit can be exceeded transiently, sometimes for several energy confinement times, before the triggering of an m=2, n=1 NTM. As q_{95} is lowered and sawteeth begin to appear, the operational β_N limit is reduced. For discharges with $q_{95} < 4$, sawteeth are universally observed in this regime and various attempts to change the scenario to avoid sawteeth have not been successful. The presence of sawteeth is correlated with a reduction in the effective β_N limit to

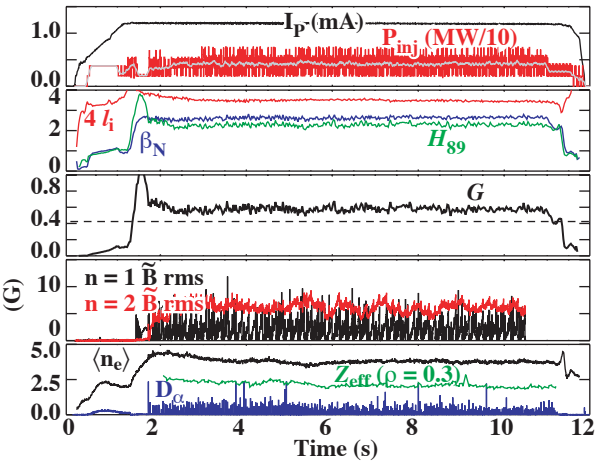

Fig. 2. Temporal evolution of a $q_{95} = 3.2$ discharge. Shown are (a) plasma current (MA) (black), actual (red) and averaged neutral beam power (grey) (MW/10) (b) internal inductance x4 (red), β_N (blue), H_{89P} (green); (c) $G \equiv \beta_N H_{89P} / q_{95}^2 l$; (d) amplitude of magnetic fluctuations at the vacuum vessel (G) for $n = 1$ (black) and $n = 2$ (red) and (e) line-average density ($10^{19}/\text{m}^3$) (black), Z_{eff} (ρ = 0.3) (green), and divertor D_α (blue). The dashed line represents the performance expected in ITER.

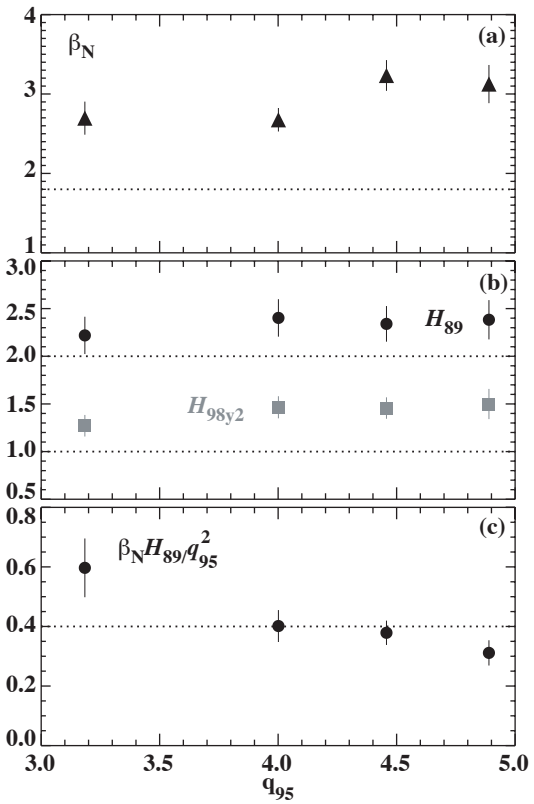

Fig. 3. Sustained (a) β_N, (b) H_{89} (black) and H_{98y2} (gray), and (c) G for during a q_{95} scan at $n_e = 5.0 \times 10^{19}$ m^{-3}.

$\beta_N \approx 2.8$. Attempts to operate at slightly higher β_N lead to a large m=2, n=1 tearing mode, which severely degrades confinement. Confinement quality over this range in q_{95} is found to be quite good relative to three confinement scalings: the aforementioned L-mode scaling, the IPB98y2 H-mode scaling [12] (denoted by H_{98y2}), and an electrostatic gyroBohm H-mode scaling derived from ITER H-mode database [13] (denoted by H_{DS03}). The latter scaling has been chosen as representative of non-dimensional scaling studies. Its primary delineation from the other scalings is lack of a strong β dependence. Confinement quality relative to the ITER89P L-mode scaling H_{89P} remains around 2.4 or 20% above the typical H-mode enhancement $(H_{89P}=2)$ while H_{98y2} and H_{DS03} are fairly constant around 1.4 with a slight drop at the lowest q_{95}. The overall performance in terms of G maximizes at low q_{95} due to the strong q_{95} dependence of G. Note that G in the high q_{95} cases is comparable to that of the ITER baseline scenario while G is approximately 50% higher than the ITER baseline scenario in the low q_{95} cases.

The variation of performance with plasma density has also been assessed. Various figures of merit from density scans at $q_{95} = 4.5$ and $q_{95} = 3.2$ are shown in Fig. 4. At $q_{95} = 4.5$, the density variation ranges from $0.3 < n_e/n_{GW} < 0.7$ while at $q_{95} = 3.2$, experiments have only been conducted in the density range $n_e/n_{GW} < 0.5$. At both q_{95} values, the sustainable β_N increases as the density is increased and is limited by the onset of an m=2, n=1 tearing mode. In the highest density case at $q_{95} = 4.5$, β_N approaches the free boundary, n = 1 stability limit. Stability calculations based on an experimental equilibrium reconstruction give $\beta_N^{no-wall} = 3.2$, very close to the experimental value. This is consistent with the presence of resistive wall modes at slightly higher β_N. Details of the stability characteristics of these discharges are discussed later. While β_N increases with density, confinement quality (relative to all scalings) decreases slightly. This decrease in confinement quality is correlated with a decrease in the ratio of the central ion temperature T_{io} to the central electron temperature T_{eo}. Nevertheless, even at $T_{io}/T_{eo} = 1.2$, confinement is observed to be enhanced relative to each of the confinement scalings with $H_{89P} = 2.1$, $H_{98y2} = H_{DS03} = 1.3$. The net result of the variations in β_N and H_{89P} is that there is little variation in G over the range of density studied.

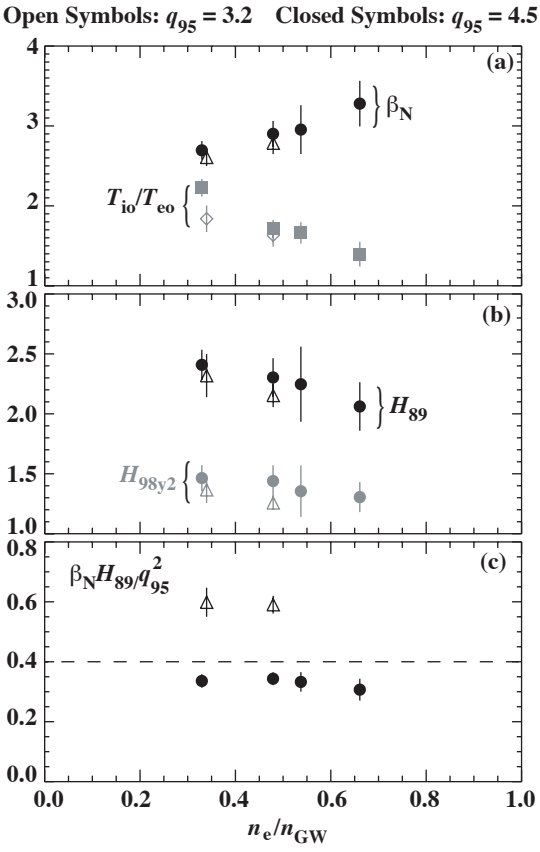

Fig. 4. (a) β_N (black) and central T_i/T_e (grey); (b) H_{89P} (black) and H_{98y2} (grey); and (c) $G \equiv \beta_N H_{89P}/q_{95}^2$ achieved in stationary conditions during a density scan at q_{95} = 4.5 (closed symbols) and q_{95} = 3.2 (open symbols). Error bars represent range of values obtained during quasi-stationary phase. ITER design values are β_N = 1.8, T_i/T_e = 1, H_{89P} = 2, H_{98y2} = 1, and G = 0.4.

As noted in the Introduction, the normalized performance of these plasmas (both in terms of performance quality and duration) significantly exceeds the performance embodied in the ITER baseline scenario. While 0-D quantities such as G and N_{τ_R} provide first-order estimates of expected performance, more reliable projections to burning plasmas require inclusion of plasma profile information. The methodology used in making these projections is discussed in Ref. [4]. These projections are uniformly positive and are given in Table I. In the q_{95} = 3.2 case, $Q_{fus} > 10$ operation with >700 MW fusion power is projected even

TABLE I. Projection of representative q_{95} = 4.4 and q_{95} = 3.2 DIII-D discharges to ITER. ITER parameters are I = 10.3 MA, β_N = 3.2, n/n_G = 0.85, B = 5.3 T at q_{95} = 4.4 and I = 13.9 MA, β_N = 2.8, n/n_G = 0.85, B = 5.3 T at q_{95} = 3.2

	q_{95} = 4.4					q_{95} = 3.2				
	H	P_{fus} (MW)	P_{aux} (MW)	Q_{fus}	t_{dur} (s)	H	P_{fus} (MW)	P_{aux} (MW)	Q_{fus}	t_{dur} (s)
ITER89P	2.75	440	49	9.0		2.4	780	60.0	12.9	
IPB98y2	1.59	440	49	8.9	3900	1.47	740	18.5	39.0	1500
Electro-static gB	1.78 (1.81)*	370	0	∞		1.25 (1.63)*	700	0	∞	

*Actual value achieved in DIII-D. The confinement multiplier must be reduced in the ignition case to obtain energy balance.

when using the pessimistic ITER89P L-mode scaling, sufficient to meet the baseline requirements of ITER's basic mission (500 MW fusion power with Q_{fus} = 10). The Ohmic solenoid in the present ITER design could sustain this for >30 min, longer than the present heat sink specification in the design can handle. Projections based on less pessimistic scaling strongly support the possibility of ignition. For example, using the electrostatic gyroBohm scaling, ignition is achieved easily and the confinement multiplier must be reduced by >20% in order to obtain energy balance. Applying the standard IPB98y2 confinement scaling, $Q_{fus} \sim 40$, and using full design current of 15 MA, ignition is marginally obtained. In the q_{95} = 4.5 case, the projection indicates that 440 MW of fusion power could be generated for pulses in excess of 1 hour, providing a fluence of ~1.0×10^{-4} MW·year/m^2 for each pulse. Remarkably, if the pure gyroBohm scaling projection were realized, ITER could achieve its baseline mission of 500 MW fusion power with $Q_{fus} > 10$ at 70% of the design current for the baseline scenario.

3. Physics Basis

As discussed previously, the limiting factor on the attainable β_N over the entire range of the operating space is the destabilization of an m=2, n=1 tearing mode, though at the high β_N values, resistive wall modes may also be playing a role. While the NTM destabilization mechanism has not been determined, the NTM onset theshold is at or above the NTM scaling prediction for the onset [14] across the entire data set. The obtained data suggests that both sawteeth and ELMs play important roles in triggering these instabilities. Empirically, avoidance of sawteeth is required to access the highest β_N values at q_{95} = 4.5 while reduced ELM size leads to improved β_N at q_{95} = 3.2. At the highest β_N values, classical destabilization of the NTM due to the rapid growth of Δ' as the free boundary, ideal stability boundary is approached [15,16] cannot be ruled out.

The lack of sawteeth in the typical q_{95} = 4.5 hybrid discharge has been discussed in detail previously [3,4,11]. These studies have suggested that the primary mechanism for maintaining $q_0 > 1$ and avoiding sawteeth is the presence of a small m=3, n=2 NTM. In the earliest studies of these discharges, analysis of the poloidal flux evolution indicated the existence of a small voltage difference (~10 mV) near the q = 1.5 surface [11]. Subsequent studies identified the modulation of the m=3, n=2 amplitude by the ELMs as a possible means of generating such a voltage [4]. In the past year, detailed studies have focused on assessing in detail the role that the m=3, n=2 mode plays in modifying the current diffusion in these discharges. An example of the differences in MHD activity when an m=3, n=2 mode is present is shown in Fig. 5(a,b). Note that in the case without an m=3, n=2 mode[Fig. 5(a)],

large sawteeth occur starting at approximately 4.0 s while in the case with an m=3, n=2 mode [Fig. 5(b)], no sawteeth are observed. Taking this one step further, recent experiments have taken advantage of the ability to control the m=3, n=2 amplitude via electron cyclotron current drive (ECCD) at the q = 1.5 surface. Controlling the m=3, n=2 amplitude is seen to have a distinct effect on the sawteeth behavior, as is shown in Fig. 5(c,d). In the co-ECCD case, the amplitude of the m=3, n=2 mode is rapidly suppressed. Soon after the m=3, n=2 mode is stabilized, large sawteeth appear and continue through the end of the discharge. In the counter-ECCD case, the discharge conditions before the application of ECCD are slightly different from the previous case such that small sawteeth are observed between 3.0-4.0 s. As the counter-ECCD is applied starting at t = 4.0 s, the m=3, n=2 amplitude increases markedly from its pre-ECCD level. Coincident with this increase, sawteeth disappear and remain dormant through the remainder of the discharge, even after the counter-ECCD has been turned off and the m=3, n=2 amplitude returns to its pre-ECCD level. Note that the estimated current drive from the ECCD is very small (<50 kA) and is therefore not expected to alter the overall current profile evolution markedly. This data, combined with previous observations, suggests that the m=3, n=2 NTM provides a sufficient reduction in poloidal flux transport that $q_0 > 1$ is maintained in stationary conditions.

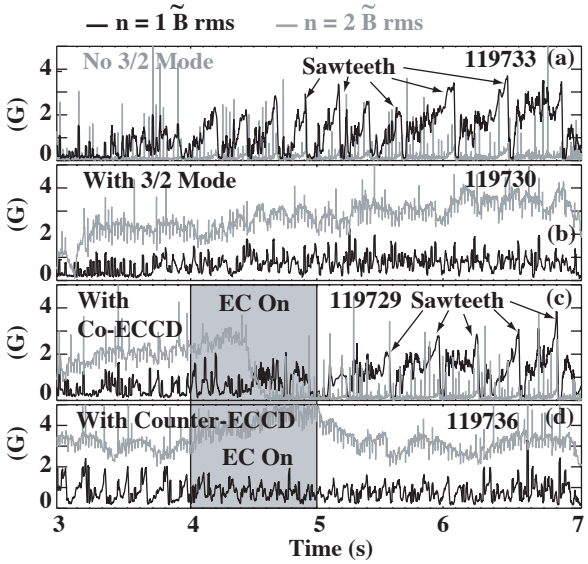

Fig. 5. Temporal evolution of magnetic fluctuation measured at the vacuum vessel (G) for n=1 (black) and n=2 (gray) for four cases: (a) a discharge without a m=3, n=2 tearing mode; (b) a discharge with a m=3, n=2 tearing mode; (c) a discharge in which co-ECCD was used to stabilize a m=3, n=2 tearing mode; and (d) a discharge in which counter-ECCD was used to enhance the amplitude of the m=3, n=2 tearing mode.

ELMs also appear to play a key role in triggering the m=2, n=1 mode in the low q_{95} cases. Although a few examples of long pulse discharges with $\beta_N > 2.5$ at $q_{95} = 3.2$ have been achieved and documented in previous papers, the reliability of achieving these conditions is very low even when the evolution of these previous discharges are matched very closely. The operating conditions (I_p = 1.2 MA, B_T = 1.2 T, ion grad B drift opposite the dominant X-point) are such that there is a narrow window for input power between the H-L threshold and the effective β_N limit. In the standard plasma shape, this results in infrequent Type I ELMs that consistently perturb the profile well beyond the q = 2 surface and have large edge pressure changes that could cause radical changes in Δ'. A possible method of improving the reliability of these discharges was revealed during experiments devoted to heating these plasmas with third harmonic electron cyclotron heating (ECH) near the plasma center. When the ECH was applied, the frequency of Type I ELMs increased markedly and $\beta_N > 2.5$ was sustained without incident until the EC power was turned off. Upon ECH turn off, the ELM frequency decreased and an m=2, n=1 NTM was destabilized within 200 ms. Based on this observation, an attempt was made to modify the ELM behavior by making subtle changes in the plasma shape via a very small change in the outer squareness δ_2 as suggested by previous results on DIII-D [17]. As in the previous experiments, increasing δ_2 resulted in a marked increase in the ELM frequency though the response in this case was much more dramatic than in the earlier experiments. An example of the differences in the ELM behavior as δ_2 is changed is shown in Fig. 6. In this discharge, a small squareness change (from δ_2 = 0.1 to δ_2 = 0.05) is performed at t = 4.0 s. At δ_2 = 0.1, the ELMs are

modest amplitude with a frequency near 30 Hz. Upon reducing the squareness to $\delta_2 = 0.05$, the ELM frequency decreases significantly while the pressure at the top of the pedestal before each ELM increases by over 50%. In most cases (the case shown in Fig. 6 being an exception), an m=2, n=1 NTM is triggered late in the $\delta_2 = 0.05$ phase by one of these large Type I ELMs. High time resolution measurements of the impurity response to these ELMs indicate that the relative ELM perturbation is nearly identical at both δ_2 values, which is consistent with the small change in the equilibrium. However, the absolute ELM perturbation is larger with $\delta_2 = 0.05$ due to the higher pedestal parameters. It should also be noted that the plasma self-inductance l_i slowly decreases throughout the $\delta_2 = 0.05$ phase, indicative of a slow radial redistribution of the current density. At this point, it is unclear whether changes in Δ' associated with the shape change (and the associated change in the pedestal pressure) or the ELM perturbation itself is responsible for the increased susceptibility of NTM destabilization at lower squareness.

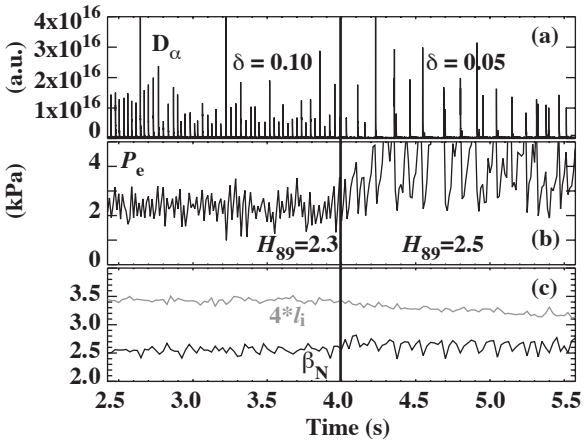

Fig. 6. Effect of a small shape change ($\delta_2 = 0.1$ to $\delta_2 = 0.05$ at 4.0 s) on the (a) upper divertor D_α signal, (b) electron pressure at the top of the pedestal, and (c) β_N (black) and $4l_i$ (gray).

As discussed previously, confinement quality in the hybrid regime is enhanced relative to the ITER89P L-mode scaling, ITER98y2 H-mode, and electrostatic gyroBohm H-mode scaling over the extent of the operation space studied to date. Although there is some degradation in confinement at the highest density levels, confinement remains good even as the ratio of the central ion and electron temperature approaches unity. Even though confinement is clearly very good in this regime, there is no evidence of internal transport barriers, as shown in Fig. 7 where profiles from the high q_{95} density scan are shown. Both the T_e and T_i profiles show signs of profile stiffness over the range of this scan as R/L_T remains nearly constant. This is consistent with GLF23 simulations that predict the profiles are unstable to both ITG and ETG modes. These GLF23 simulations also suggest that ExB shear stabilization is an important ingredient in reproducing the measured temperature profiles [18]. A sample comparison between the simulation (with and without ExB stabilization included) and the measured profiles is shown in Ref. [18]. The agreement between the simulation and the measured data is found to be substantially improved with ExB stabilization included. This prediction is qualitatively consistent with experimental cases under identical conditions but different rotation profiles. All of data in the high q_{95} density scan was obtained with the DIII-D error correction coils disabled to facilitate high β_N access (for reasons not yet understood).

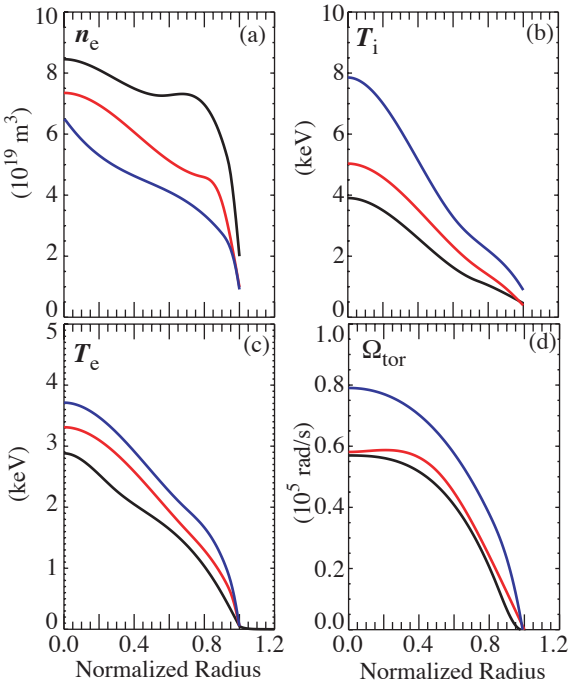

Fig. 7. Profiles of (a) n_e, (b) T_i, (c) T_e, and (d) Ω_{tor} during a density scan at $q_{95} = 4.5$.

Therefore, intrinsic error fields are present in these shots and the obtained rotation is significantly lower than obtained with proper error correction applied. In cases with proper error field correction applied (and therefore higher rotation), confinement is markedly better. In the best cases, with $H_{89P} = 2.8$, $H_{98y2} = H_{DS03} = 1.7$. Yet, even at rotation frequencies less than 10^5 rad/s without error field correction applied, overall confinement is still better than the standard H-mode scalings over the entire range of this density scan.

4. Summary

In summary, a new standard in stationary tokamak operation is emerging from recent studies on the DIII-D tokamak. These studies have demonstrated the ability to operate near the free boundary, n = 1 stability limit with good confinement quality for durations in excess of three resistive diffusion times. In addition, the operation space has been shown to be extensive, ranging from $0.35 < n_e/n_{GW} < 0.7$ and edge safety factor $3.0 < q_{95} < 4.5$. Performance in most cases is limited by the onset of m=2, n=1 NTMs triggered by either sawteeth or ELMs. Nevertheless, the normalized performance figure of merit G in these discharges exceeds that of the ITER baseline scenario over the entire operating range. Projections to ITER based on the obtained results are uniformly positive and suggest a range of operating options for ITER, ranging from $Q_{fus} >> 10$ operation at full engineering parameters to long pulse, $Q_{fus} = 5$ operation at reduced engineering parameters. While this regime shares many of the same characteristics as the conventional H-mode regime, several important aspects that distinguish this regime have been elucidated. Studies have shown that the sawteeth amplitude in these discharges is reduced by the presence of an m=3, n=2 NTM, which acts to raise q_0 above 1. In addition, the effect of ELMs on NTM destabilization has been reduced by subtle changes in the plasma shape. Finally, comparisons of obtained data with transport simulations indicate that ExB stabilization plays an important role in reducing ITG-driven turbulence, though turbulent-driven transport is still present for both the ions and electrons. Yet, even in cases in which ExB stabilization is not predicted to be important, confinement quality is improved relative to the relevant confinement scalings.

Acknowledgment

This work was supported by the U.S. Department of Energy under DE-AC05-00OR22725, DE-FC02-04ER54698, W-7405-ENG-48, and DE-FG03-01ER54615.

References

[1] ITER Physics Basis, Editors, Nucl. Fusion **39** (1999) 2137.
[2] WADE, M.R., *et al.,* Proc. 29th EPS Conf. on Plasma Phys. and Control. Fusion, Montreux, 2002, Vol. **26B** (ECA) O-2.08.
[3] LUCE, T.C., *et al.,* Nucl. Fusion **43** (2003) 321.
[4] LUCE, T.C., *et al.,* Phys. Plasmas **11** (2004) 2627.
[5] SIPS, A.C.C., *et al.,* Plasmas Phys. Control. Fusion **44** (2002) B69.
[6] JOFFRIN, E.H., *et al.,* Plasmas Phys. Control. Fusion **45** (2003) A367.
[7] ISAYAMA, A., *et al.,* Nucl. Fusion **43** (2003) 1272.
[8] AYMAR, R., BARABASCHI, P., SHIMOMURA, Y., Plasma Phys. Control. Fusion **44** (2002) 519.
[9] YUSHMANOV, P.N., *et al.,* Nucl. Fusion **30** (1990) 1999.
[10] MIKKELSEN, D.R., Phys. Fluids B **1** (1989) 333.
[11] WADE, M. R., *et al.,* Phys. Plasmas **8** (2001) 2208.
[12] ITER Physics Basis Editors, ITER Physics Expert Group Chairs and Co-Chairs, ITER Joint Central Team and Physics Integration Unit, Nucl. Fusion **39** (1999) 2137.
[13] PETTY, C.C., *et al.*, Fusion Sci. Tech. **43** (2003) 1.
[14] HENDER, T.C., *et al.*, Nucl. Fusion **44** (2004) 788.
[15] BRENNAN, D.P., *et al.,* Phys. Plasmas **10** (2003) 1643.
[16] PETTY, C.C., *et al.*, this conference.
[17] FERRON, J.R., *et al.,* Phys. Plasmas **7** (2000) 1976.
[18] KINSEY, J.E., *et al.,* this conference.